Journal of Pharmaceutical and Biomedical Analysis 246 (2024) 116204

Contents lists available at ScienceDirect

Journal of Pharmaceutical and Biomedical Analysis

journal homepage: www.journals.elsevier.com/journal-of-pharmaceutical-and-biomedical-analysis

To elucidate the bioactive components of Lamiophlomis herba in the treatment of liver fibrosis via plasma pharmacochemistry and network pharmacology

Jiaming Ge [a,b,c,1], Weisan Chen [a,1], Mengyuan Li [b,c], Jing Zhao [b,c], Ying Zhao [a,b], Jiali Ren [a,b], Xinchen Gao [a,b], Tianbao Song [a,b], Xiankuan Li [a,b,d,*], Jinlong Yang [d,**]

[a] School of Chinese Materia Medica, Tianjin University of Traditional Chinese Medicine, Tianjin 301617, China
[b] Tianjin Key Laboratory of Therapeutic Substance of Traditional Chinese Medicine, Tianjin 301617, China
[c] College of Pharmaceutical Engineering of Traditional Chinese Medicine, Tianjin University of Traditional Chinese Medicine, Tianjin 301617, China
[d] State Key Lab of New Ceramics and Fine Processing, School of Materials Science and Engineering, Tsinghua University, Beijing 100084, China

ARTICLE INFO

Keywords:
Lamiophlomis herba
Liver fibrosis
Bioactive components
Plasma pharmacochemistry
UPLC-Q-TOF-MS
Network pharmacology

ABSTRACT

Lamiophlomis Herba (LH) is a traditional Chinese and Tibetan dual-use herb with hemostatic and analgesic effects, and is widely used in the clinical treatment of traumatic bleeding and pain. In recent years, LH has been proven to treat liver fibrosis (LF), but the chemical components related to the pharmacological properties of LH in the treatment of LF are still unclear. Based on the theory of plasma pharmachemistry, the characteristic components in water extract and drug-containing plasma samples of LH were qualitatively analyzed by UPLC-Q-TOF-MS. The chemical components in plasma were screened and the targets were predicted by network pharmacology. Then, the predicted components and targets were verified in vitro by Elisa and qRT-PCR technology. Finally, the pharmacological effects of LH and its monomeric components were determined by hematoxylin-eosin staining of rat liver. A total of 50 chemical constituents were identified in LH, of which 12 were blood prototypes and 9 were metabolites. In vitro experiments showed that LH and its monomeric components luteolin, shanzhiside methyl ester, loganic acid, loganin, 8-O-acetyl shanzhiside methyl ester could increase the expression of antioxidant genes (NQO-1, HO-1) and decrease the expression of inflammatory genes (IL-6, IL-18), thereby reducing the expression of extracellular matrix-related genes and proteins (COL1A1, COL3A1, LN, α-sma, PC-III, Col-IV). In vivo experiments showed that LH could reduce the area of LF in rats in a dose-dependent manner, and shanzhiside methyl ester and 8-O-acetyl shanzhiside methyl ester may be the main components in pharmacodynamics. These effects may be mediated by LH-mediated Nrf2/NF-κB pathway. This study explored the potential pharmacodynamic components of LH in the treatment of LF, and confirmed that shanzhiside methyl ester and 8-O-acetyl shanzhiside methyl ester play a key role in the treatment of LF with LH.

1. Introduction

Liver fibrosis (LF) is a pathophysiological process triggered by multiple factors. Failure to administer timely treatment can lead to the progression of cirrhosis and hepatocellular carcinoma [1]. LF primarily arises from the activation and proliferation of hepatic stellate cells (HSCs), resulting in the generation of myofibroblasts, which are induced by various inflammatory factors, predominantly TGF-β1 and PDGF. The activation of HSC by TGF-β1 prompts the secretion of extracellular matrix-related proteins and tissue inhibitor of metalloproteinases through the stimulation of the TGF-β signaling pathway, ultimately leading to LF development [2]. Bone marrow-derived mesenchymal stem cells undergo epithelial-mesenchymal transition to differentiate into myofibroblasts, thereby providing a complementary mechanism for inducing LF [3]. In accordance with traditional Chinese medicine (TCM) theory, LF manifests as blood stasis. Hence, herbal remedies that promote blood circulation by removing stasis are commonly employed for its treatment [4].

* Correspondence to: 10 Poyanghu Road, West Area, Tuanbo New Town, Jinghai District, Tianjin, 301617, China.
** Correspondence to: 30 Shuangqing Road, Haidian District, Beijing, 100084, China.
E-mail addresses: lixiankuan@tjutcm.edu.cn (X. Li), jlyang@mail.tsinghua.edu.cn (J. Yang).
[1] Jiaming Ge and Weisan Chen contributed equally to this work.

https://doi.org/10.1016/j.jpba.2024.116204
Received 31 January 2024; Received in revised form 30 April 2024; Accepted 5 May 2024
Available online 17 May 2024
0731-7085/© 2024 Elsevier B.V. All rights are reserved, including those for text and data mining, AI training, and similar technologies.

Lamiophlomis Herba (LH) is desiccated aboveground portion of *Lamiophlomis rotata* (Benth.) Kudo. It is recorded that LH has the effect of activating blood and dissolving stasis, clearing wind-damp for relieving pain and arrest bleeding in ancient Chinese and Tibetan medicine pharmacopeia [5]. Recent pharmacological studies have shown that total polyphenolic glycosides (TGP) in LH promote apoptosis of activated HSCs, downregulate the expression of Smad2/Smad3, Smad4 and upregulate the expression of Smad7 in mice with LF, thereby inhibiting the TGF-β1 signalling pathway and reducing the expression of related extracellular matrix-forming proteins [6]. In addition, TGP promotes the conversion of activated HSC to inactivated HSC by inhibiting AGE/R-AGE [7]. However, the specific bioactive compounds within polyphenolic glycosides that are responsible for exerting their pharmaceutical effects remain unidentified. The main polyphenols in LH are iridoids, flavonoids and small amounts of phenolic acids, and some phenylpropanoids are also found in LH [5]. The iridoids and flavonoids present in LH exhibit anti-inflammatory and analgesic effects, while the phenylpropanoids have been substantiated for their remarkable anti-inflammatory and antibacterial properties [5]. The activation of HSCs is facilitated by IL-6 through the regulation of the HIF/IL-6/STAT3 signaling pathway, while NLRP3 inflammasome activation induced by IL-18 triggers HSC activation [8,9]. As an activator of inflammatory pathways, reactive oxygen species (ROS) can be inhibited by HO-1 and NQO-1 [10]. The Nrf2-cascaded NF-κB pathway exerts regulatory control over the generation of ROS and pro-inflammatory factors. LH may play an antioxidant and anti-inflammatory role in the treatment of LF by mediating Nrf2/NF-κB pathway.

Therefore, in this study, the UPLC-Q-TOF-MS technology was employed to identify and characterize the constituents of LH as well as their absorption into the bloodstream. Utilizing plasma pharmacochemistry results, network pharmacology was applied to construct a multi-level network relationship between the "active ingredient-target-pathway" of LH in treating LF. Subsequently, the antioxidant and anti-inflammatory targets predicted by network pharmacology in LR were verified by in vitro experiments. Finally, morphologic examination of rat liver tissue was performed to validate the role of LH and its monomeric components, SME and 8-OASME, in ameliorating LF. These findings are expected to serve as a foundation for further exploration of LH's bioactive ingredients and mechanism in managing LF.

2. Materials and methods

2.1. Drugs and reagents

LH was purchased from Anguo traditional Chinese medicine professional market (Hebei, China). Silymarin capsules (Positive control; P-control) were purchased from MADAUS GMBH (Cologne, Germany). Standards of shanzhiside methyl ester (SME) ≥ 98 %, 8-O-acetyl shanzhiside methyl ester (8-O ASME) ≥ 98 %, loganin (Log) ≥ 98 %, loganic acid (Log A) ≥ 98 % and luteolin (Lut) ≥ 98 % were purchased from Shanghai Yuanye Bio-Technology Co., Ltd. (Shanghai, China) (Fig. 1). Recombinant Mouse/Rat TGF-beta 1 was provided by Suzhou Nearshore Protein Technology Co., Ltd. (Suzhou, China). Formic acid (MS grade) and acetonitrile (HPLC grade) were obtained Merck (Darmstadt, Germany). DMEM culture chamber and fetal bovine serum (FBS) were obtained from GIBCO BRL (Grand Island, NY, USA). Penicillium-streptomycin, trypsin, and PBS buffer were obtained from Beijing Solarbio Science & Technology Co., Ltd. (Beijing, China). Purified water was supplied by A.S. Watson TM LIMITED (Guangzhou, China).

2.2. Preparation of LH extract

100 g LH was soaked in 1600 mL water for 30 min, and then decocted for 30 min. After filtration, 1400 mL water was added to the filter residue and decocted again for 20 min. Samples were filtered through 0.22 μm microporous filters before analysis. Finally, the water extract of LH was obtained and concentrated to 50 mL, equivalent to 2 g/mL of crude medicine for subsequent experiments. According to the Pharmacopoeia of the People's Republic of China, combined with our previous research, qualitative and quantitative analysis was conducted on LH water extract, which was identified as the dried aboveground part of *Lamiophlomis rotata* (Benth.) Kudo. The concentrations of SME and 8-O ASME were determined to be 20.4 mg/mL and 21.6 mg/mL, respectively [11] (Figure S1).

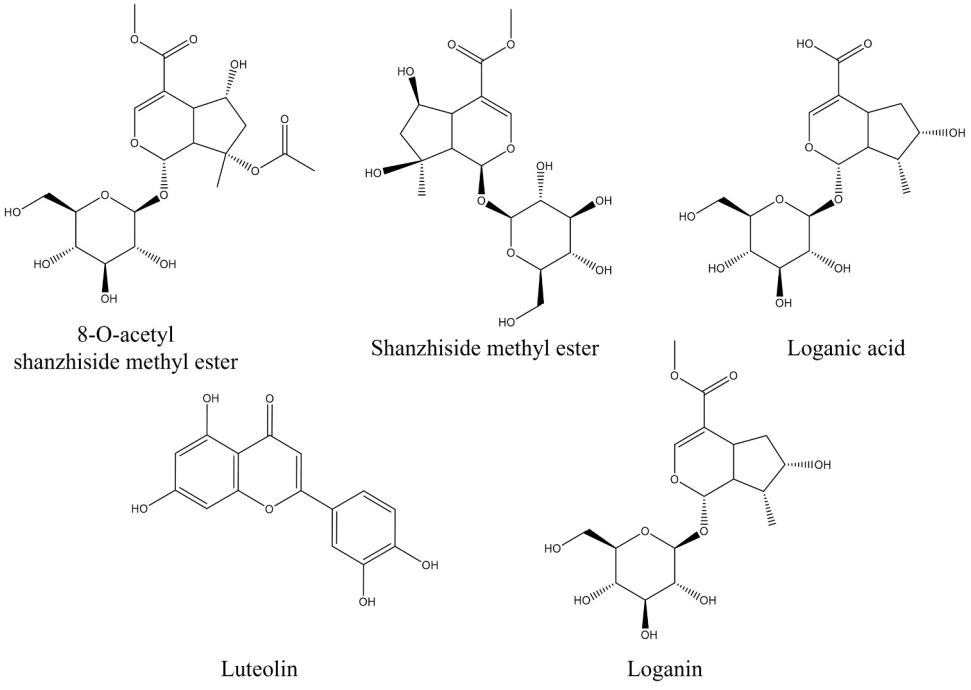

Fig. 1. Chemical structures of the five compounds.

2.3. Animal

Male Sprague Dawley (SD) rats (200 ± 20 g) were obtained from Beijing Huafukang Biotechnology Co., Ltd. (Beijing, China), and the rearing of experimental animals was approved by Tianjin University of Traditional Chinese Medicine and performed in accordance with ethical standards (Animal Ethics No.: TCM-LAEC202113). The rats were housed in an animal center (22 ± 2℃, 60 ± 10 % relative humidity), following a 12-hour light/dark cycle. They had ad libitum access to food and water, except for a 24-hour fasting period prior to the experiment during which they had free access to water.

2.4. Preparation of plasma samples

12 male SD rats were randomly divided into blank group (6 rats) and LH group (6 rats). The dosage for intragastric administration was determined based on the acute toxicity experiments conducted by Wang et al. and Zhang et al., with a safe dose established to be below 18 g/kg in rats [12]. Considering the appropriate volume for rat dosing, the final concentration for intragastric administration was set at 15 g/kg. Rats in the LH group were administered 15 g/kg of an aqueous extract of LH intragastrically, while rats in the blank group received an equivalent volume of 0.9 % NACl solution. Blood samples were collected from the orbital plexus vein at 0.5, 1, 2, 4 and 6 h after administration and transferred to heparinized centrifuge tubes. Subsequently, plasma was separated by centrifugation at 4℃ and 3000 r/min for 15 min before being stored at −80℃.

The same treatment protocol was used for the blank and LH groups. After plasma absorption of 50 μL at each time point, 500 μL of acetonitrile was added, thoroughly mixed, and then centrifuged at 4℃ for 10 min at 12000 r/min, and the supernatant was collected. The solution was blow-dried with nitrogen, and the residue was redissolved in 200 μL acetonitrile. Samples were filtered through 0.22 μm microporous filters before analysis.

2.5. Chemical composition and plasma composition analysis

The water extract of LH and plasma samples from the blank and LH group were analyzed by UPLC-Q-TOF-MS. Chromatographic analysis was performed using a Waters Acquity™ UPLC system (Waters Corporation, Milford, USA). The 1 μL sample were separated on a Waters Acquity UPLC HSS T_3 column at 45℃ with a flow rate of 0.3 mL/min. The mobile phases A (0.1 % formic acid in water) and B (0.1 % formic acid in acetonitrile) were set as follows: 0–2 min, 1–10 %B; 2–5 min, 10–15 %B; 5–8 min, 15–20 %B; 8–10 min, 20–25 %B; 10–13 min, 25–35 %B; 13–18 min, 35–99 %B; 18–20 min, 99 %B; 20–22 min, 99–1 %B; 22–25 min, 1 %B.

Water Xevo G_2 Q-TOF mass spectrometer (Waters Corporation, Milford, USA) was used for negative mode scanning determination equipped with an electrospray ionization (ESI), and the instrument parameters were as follows: The data was acquired using a capillary voltage of 2.0 kV (ESI-), cone-hole voltage of 30 V, ion source temperature of 110℃, cone-hole gas flow rate of 50 L/h, quality data collection scan of 50–1200 Da. Leucine enkephalin was used for real-time molecular weight correction during the collection process.

2.6. Network pharmacology analysis

2.6.1. Ingredients targets screening

Based on the results of chemical analysis and the components of LH absorbed in rat plasma, the prototype and metabolic compounds absorbed in rat plasma were selected as candidates. The determination of the targets on LH by TCMSP Database (http://old.tcmsp-e.com/tcmsp.php) and SwissTargetPrediction (http://www.swisstargetprediction.ch/). Besides, the molecular targets of some known identified compounds were collected through literature mining. Merge all targets and remove duplicates.

2.6.2. Liver fibrosis related target collection

Targets of LF were identified by searching public databases, including Online Mendelian Inheritance in Man (OMIM, https://omim.org/), Therapeutic Target Database (http://db.idrblab.net/ttd/), GeneCards (https://www.genecards.org/), DisGeNET (http://www.disgenet.org/) and remove duplicate targets. Next, overlapping genes between LH and LF were matched to Venn diagrams.

2.6.3. Construction of "component-target-pathway" network and analysis of key targets and pathways

Cytoscape 3.8.2 software was used to construct the active compound-disease target network to describe the interaction between target genes and bioactive components. The degree values were subsequently calculated using the NetworkAnalyzer plug-in. Compounds with higher values in LH are considered to be potentially active compounds that may be involved in LH-mediated remission of LF. The DAVID database was used to perform KEGG pathway and GO function enrichment analysis of gene targets. Terms with $P < 0.05$ were considered significant and captured for revealing the related pathways and metabolic processes involved in the treatment of LH on LF.

2.7. Cell experiment

2.7.1. Cell preparation and stimulation

Rat hepatic stellate cells (HSC-T6) were purchased from the Procell Life Science&Technology Co., Ltd. (Wuhan, China). Cells were cultured in DMEM supplemented with 10 % fetal bovine serum and 1 % penicillin and streptomycin at 37℃ with 5 % CO_2. Cells in the logarithmic growth phase were used for further experiments. The cells were divided into control, model, P-control (8 μg/mL), SME (40 μM/L), 8-O ASME (40 μM/L), Log (10 μM/L), Log A (10 μM/L), Lut (80 μM/L) and LH water extract (LH-L: 400 mg/L, LH-M: 800 mg/L, LH-H: 1600 mg/L) and cultured for 12 h for further experiments. Except for the control group, the culture medium of other groups contained 5 ng/mL TGF-β1. The administration concentration and cytotoxicity were assessed using a combination of MTT assay and LDH experiments. The experimental findings are presented in Figure S1.

2.7.2. Elisa

Elisa kits of laminin (LN), type IV collagen (Col-IV), type III procollagen (PC-III) and smooth muscle protein (α-sma) were purchased from Jiangsu Meimian Industrial Co., Ltd. (Yangcheng, China), according to the manufacturer's instructions to experiment.

2.7.3. qRT-PCR

The mRNA expression of GAPDH, NQO-1, HMOX-1, IL-6, IL-18, Col3a1 and Col1a1 were detected by qRT-PCR. Total RNA was extracted from HSC-T6 cells using TRNzol kit and the concentration of extracted RNA was detected using Nano-400A ultra micro nucleic acid analyzer. cDNA synthesis was performed with 600 ng of total RNA using a FastKing cDNA first strand Synthesis Kit with gDNase. Quantitative real-time PCR (qRT-PCR) analysis was performed using a SuperReal fluorescence quantitative premix reagent in an CFX96 fluorescence quantitative PCR instrument. These kits were purchased from Tiangen Biochemical Technology Co., LTD (Beijing, China). GAPDH was analyzed in each sample to normalize expression. The primers used are shown in Table S1.

2.8. Animal experiment verification

2.8.1. Liver fibrosis model

According to the prediction results of network pharmacology and cell experiment, combined with the previous experiments and pharmacopoeia standards, SME and 8-O ASME were selected for animal

experiment verification [11]. 96 rats were randomized into 8 groups (n = 12), the control group received intraperitoneal injections of olive oil, while the remaining groups received a solution containing 50 % CCl4 in olive oil (2.0 mL/kg) twice weekly for 8 weeks. According to the clinical equivalent dose and the content of components in the water extract, the dosages of LH-L, LH-M, and LH-H groups were 0.3, 0.6, and 1.2 g/kg, respectively, and the dosages of SME and 8-O ASME were 10 mg/kg. The control and model groups received the same amount of 0.9 % NaCl solution by gavage administration.

2.8.2. Hematoxylin and eosin stain of liver

Liver tissues were immersed in 4 % paraformaldehyde, dehydrated in ethanol, embedded in paraffin, and sectioned at 5 μm. The sections were stained with hematoxylin and eosin (HE), dehydrated through a gradient, and sealed with neutralresinsize. Changes in liver tissues were observed under a microscope, and image acquisition and analysis were performed.

2.9. Statistical analysis

Statistical analysis was performed using GraphPad Prism 9.0 software (Version 23.0; IBM SPSS, Chicago, Illinois, USA). The results were expressed as mean ± SD and each experiment was repeated 3 times. One-way analysis of variance (ANOVA) was used to evaluate the differences in the mean values. The significance difference was verified by Tukey-Kramer honesty ($P < 0.05$).

3. Results

3.1. Identification of chemical compositions in LH

UPLC-Q-TOF-MS analysis was used to identify the compounds in LH. Since MS and ion fragment information are more informative in the negative ion mode, analyses were performed in the negative ion mode. To identify the compounds in LH, the retention time, excimer ions, and ion fragments of the obtained mass spectra were analyzed and compared with those reported in the database. By comparison with the database, a total of 50 compounds were identified, including 9 flavonoids, 19 phenylpropanoids, 20 iridoids and 2 other compounds. The results and mass spectra of these compounds are shown in Fig. 2-A and Table S2.

The cleavage of iridoids is characterized by dehydration, decarboxylation, desugarization and occasionally ring opening (Fig. 3). The quasi-molecular ion peak of compound 28 is *m/z* 493.1563 $[M+COOH]^-$. It loses a glucose group (162 Da) to form an ionic fragment of *m/z* 285 $[M-Glu]^-$, which is then cleaved into two fragments of *m/z* 225 and *m/z* 101. Another cleavage involves the loss of a methoxy group (30 Da) and a glycolic acid (59 Da) to form an ionic fragment of *m/z* 359, which is then cleaved into a fragment of *m/z* 323. Based on a comparative analysis of the data from previous literature, we postulate that this compound corresponds to 8-O ASME [13].

The quasi-molecular ion peak of compound 24 is *m/z* 435.1493 $[M+COOH]^-$. The compound first shows loss of a glucose group (162 Da) to form the fragment *m/z* 227 $[M-H-Glu]^-$, followed by successive loss of two water molecules (36 Da) to form the fragment *m/z* 191 $[M-H-Glu-2\ H_2O]^-$, and then loss of a methoxy group (30 Da) to form the characteristic peak of *m/z* 161 $[M-H-Glu-2\ H_2O-OCH_2]^-$. According to the literature of Wu et al., the compound is consistent with the cleaved law of Log, so it is inferred that it is Log [14].

The characteristic quasi-molecular ion peak of compound 11 is observed at *m/z* 451.1452 $[M+COOH]^-$, indicating the loss of a glucose group at *m/z* 243 $[M-H-Glu]^-$, followed by subsequent losses of C_2H_4 (28 Da) and H_2O (18 Da), resulting in the formation of ion fragments at *m/z* 215 $[M-H-Glu-C_2H_4]^-$ and *m/z* 225 $[M-H-Glu-H_2O]^-$. According to the data in previous literatures, this compound is inferred to be SME [13].

Lut and quercetin are the basic backbone of flavonoids in LH to form glycosides. During cleavage, the saccharides are mainly removed to form aglycones, and further occurs Retro Diels-Alder (RDA) reaction (Fig. 4). The quasi-molecular ion peaks of compounds 31, 32, and 48 were observed at *m/z* 579.1350 $[M-H]^-$, *m/z* 447.0927 $[M-H]^-$, and *m/z* 285.0399 $[M-H]^-$, respectively. These compounds exhibited characteristic fragments at *m/z* 285, consistent with the presence of Lut. Compounds 31 and 32 produced ions at *m/z* 447 (132 Da) and *m/z* 285 (162 Da), respectively, indicating continuous glycosidic bond cleavage. Compound 48 showed two fragments at *m/z* 155 and *m/z* 131, consistent with the RDA cleavage pattern of Lut. By comparing these results with the identification of flavonoids in LH by La et al., it can be concluded that compounds luteolin-7-O-(6''-O-β-D-apiofuranosyl)-β-D-glucopyranoside, luteolin-7-O-β-D-Glucoside, and Lut correspond to compounds 31, 32, and 48 [13,14].

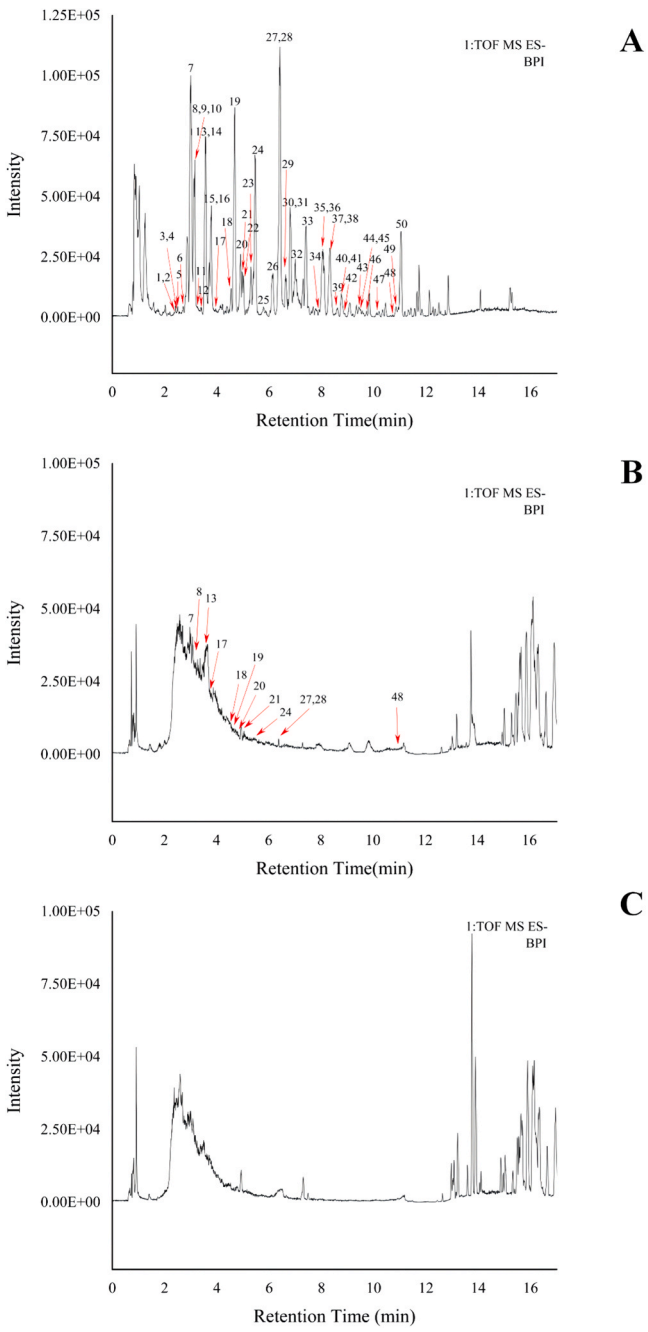

Fig. 2. Diagram of the total ion current in the negative ion mode. (A: Aqueous extract of LH; B: LH group plasma sample; C: Blank group plamsa sample).

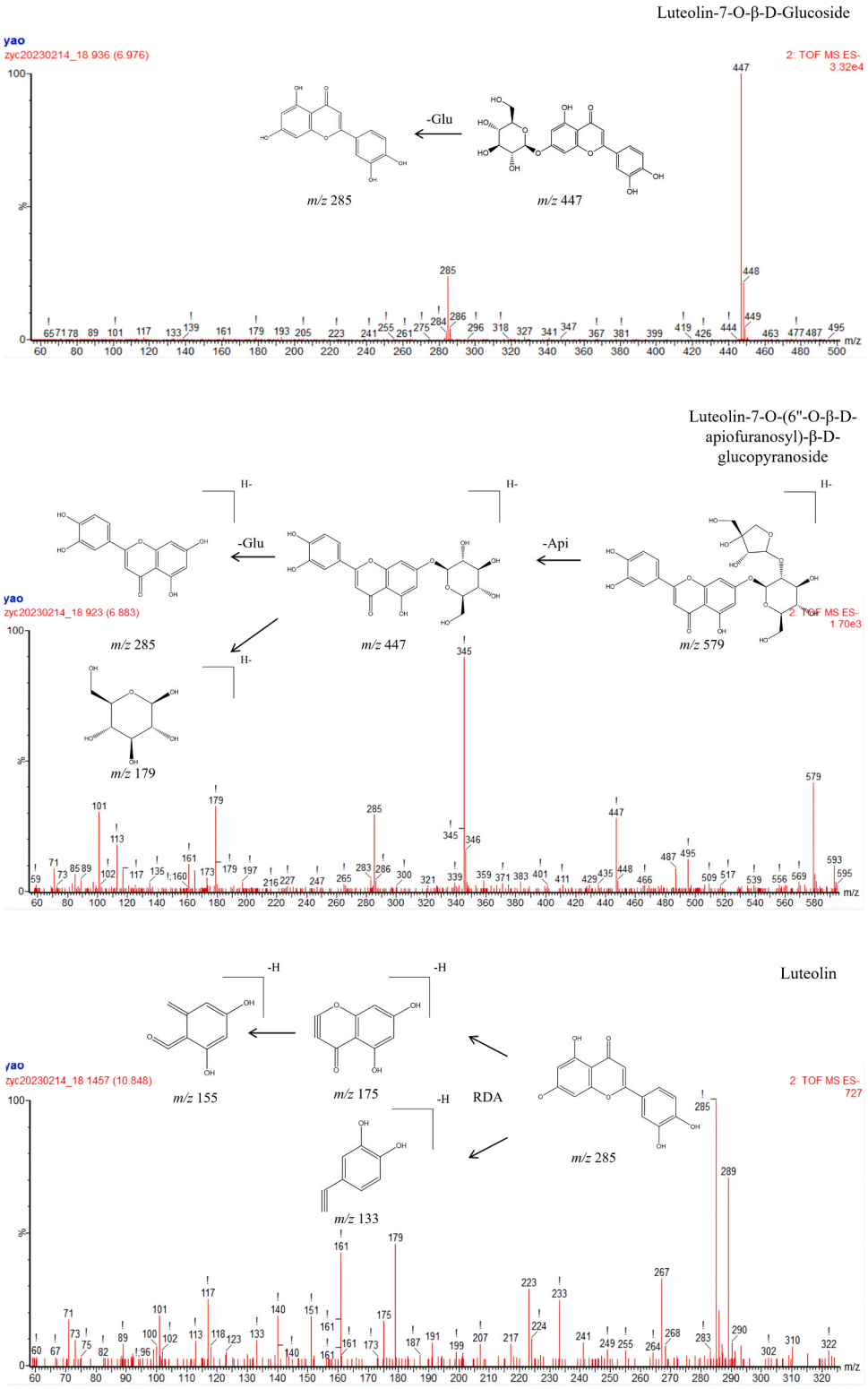

Fig. 3. The cleavage rule of iridoids. (Compound 11, 24, 28).

Phenylpropanoids are one of the most abundant components in LH, mainly composed of phenylpropanol compounds, but also contain a small amount of phenylpropionic acid compounds. The cleavage pathway of phenylpropanoid compounds is mainly related to the group connected on the parent nucleus, including the loss of methyl, hydroxyl, carboxyl and others (Fig. 5). The quasi-molecular ion peak of compound 14 is observed at *m/z* 353.0873 $[M\text{-}H]^-$, with two characteristic fragments detected at *m/z* 191 and *m/z* 179, corresponding to the loss of quinonic acid (174 Da) and caffeic acid (162 Da), respectively. Subsequently, these fragments underwent dehydration reactions resulting in the formation of characteristic ions at *m/z* 173 and *m/z* 161. By comparing our results with previously reported data, it can be concluded that the compound under investigation is chlorogenic acid [14].

The quasi-molecular ion peak of compound 33 is observed at *m/z*

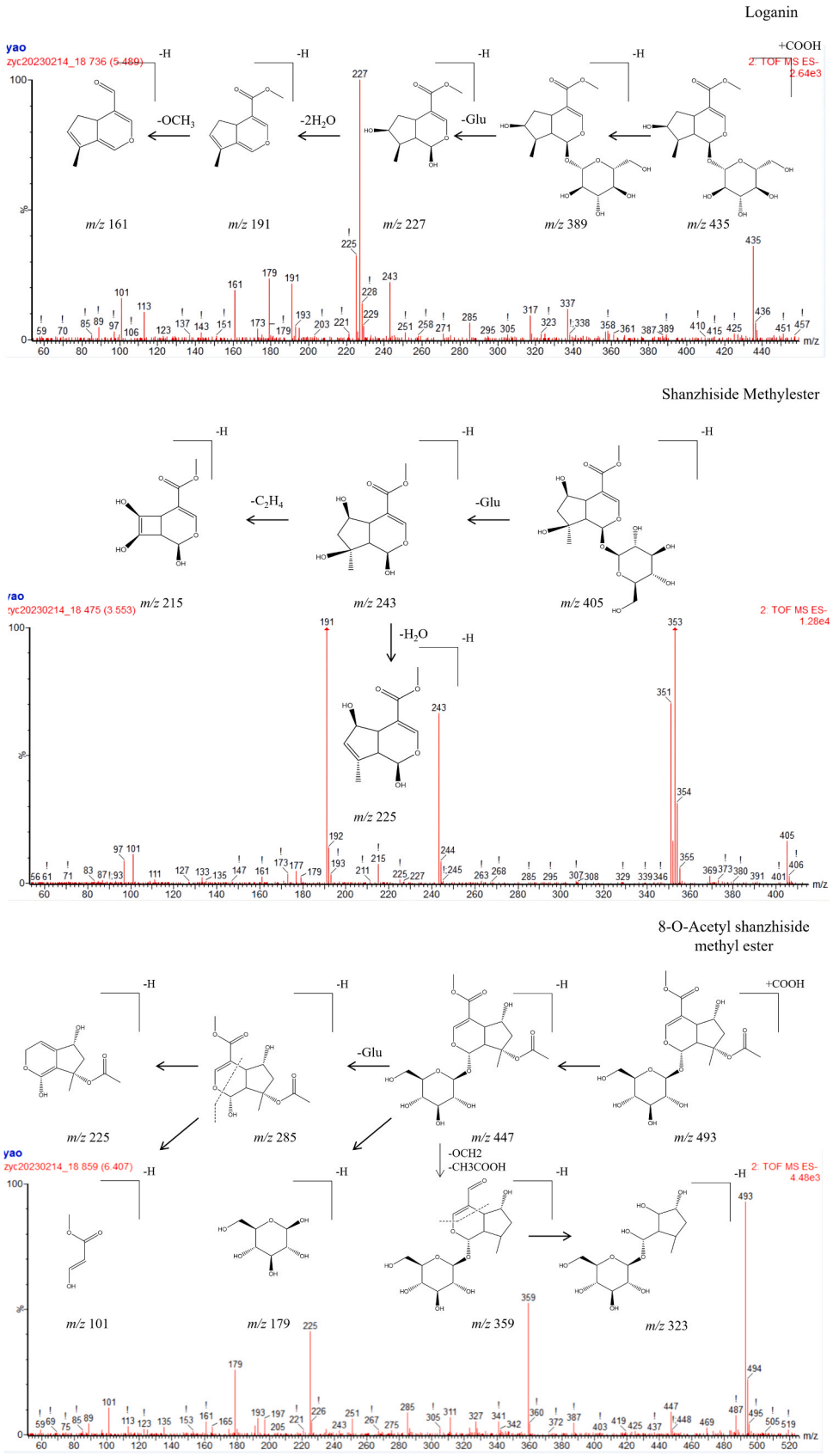

Fig. 4. The cleavage rule of flavonoids. (Compound 31, 32 and 48).

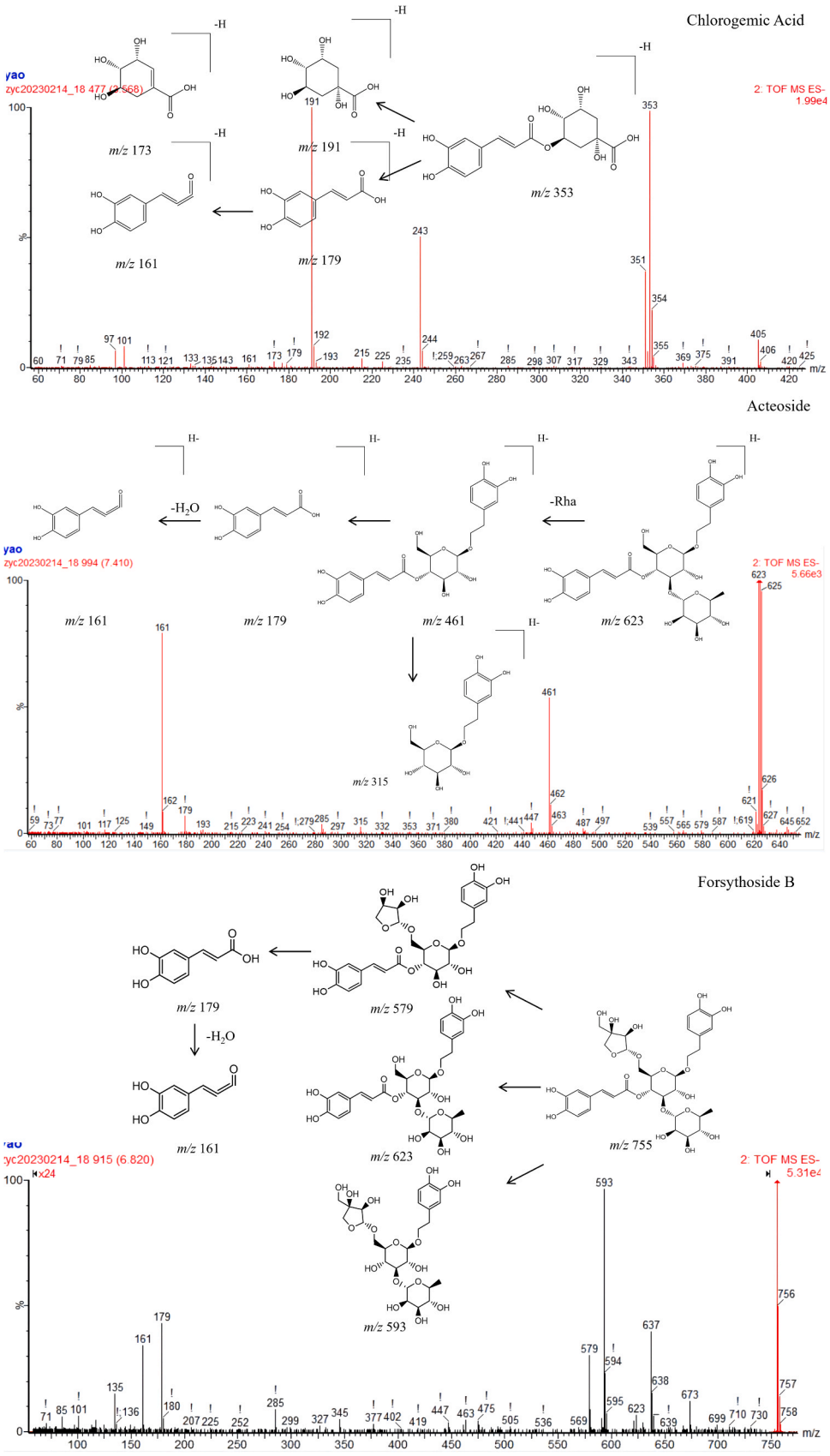

Fig. 5. The cleavage rule of phenylpropanoids. (Compound 14, 30, 33).

623.1976 [M-H]$^-$. The compound first loses 162 Da to form a fragment ion at *m/z* 461 [M-H-Rha]-, corresponding to the removal of a rhamnose moiety. Subsequent cleavage of the glycosidic bond produces two fragment ions at *m/z* 179 and *m/z* 315, respectively, and then a molecule of H_2O is lost, producing a fragment ion at *m/z* 161. The compound is consistent with the compound known as acteoside found in LH by Wu et al. It is concluded that the compound is acteoside [14].

The excimer peak of compound 30 is *m/z* 775.2399, and four characteristic peaks are observed at *m/z* 579, *m/z* 623, *m/z* 593, and *m/z* 179, indicating fragments formed by the rupture of different sites of glycosidic bond, followed by fragments formed by dehydration at *m/z* 161, and then fragments formed by the rupture of C-C double bond at *m/z* 135. In agreement with the data of Wu et al., this compound is inferred to be Forsythoside B [14].

In addition to the compound types proposed above, we also found syringic acid and vanillyl-β-d-Glucopyranoside in LH. The cleavage pathway of these compounds mainly includes the loss of hydroxyl, carboxyl, methoxy.

3.2. Identification of components of LH into rat plasma

The BPI plots of the negative control group and the drug administration group are shown in Figs. 2-B and 2-C. By comparison with the compounds identified in the aqueous extract of LH, a total of 12 prototype components were identified. The identification results and fragment ion are shown in Table 1.

The identification of metabolic components in LH was achieved by considering the retention time of the prototype compound, the fragmentation behavior, and the metabolic transformation patterns exhibited by compounds sharing the same parent nucleus structure. The first-phase metabolism is mainly demethylation, oxidation and hydrolysis, while the second-phase metabolism is combination with endogenous components, including glucuronidation, sulfonation and acetylation (Table 2).

Lut, a prevalent flavonoid in food and herbal medicines, was found to yield five metabolites in this study. Due to the ubiquitous presence of UDP-glucuronosyltransferase (UGT) and catechol-O-methyltransferase (COMT) enzymes in the body, glucuronidation and methylglucuronidation products of Lut are frequently detected in vivo [15].

The M8 displayed an ion at *m/z* 475.0877 [M-H]$^-$ and an ion peak at *m/z* 299.0597 (loss of a glucuronate), followed by the elimination of a methyl group, which corresponded to the quasi-molecular ion of Lut (*m/z* 285.0410). Subsequently, the same ring cleavage fragment as that observed in Lut was identified, including loop A (*m/z* 151.0007) and B (*m/z* 133.0301). By comparing the data with the relevant literature, we concluded that the product was the methyl glucuronidation product of Lut. The quasi-molecular ion peak of M7 is observed at *m/z* 364.9967 [M-H]$^-$, which has a mass difference of 14 Da compared to that of M8. The cleavage rule are consistent with those detected for M8, suggesting that M7 is the glucuronidation product of Lut [15].

Furthermore, we found the quasi-molecular ion peaks of M2 (*m/z* 637.1041 [M-H]$^-$), M6 (*m/z* 541.0288 [M-H]$^-$) and M9 (*m/z* 364.9967 [M-H]$^-$) in our study, which underwent sequential desulfation or deglucuronidation to generate the parent nucleus structure of Lut. The observed cleavage patterns were consistent with previous literature reports, so we concluded that they were the double-glucuronidized, sulfate-glucuronidized, sulfated metabolites of Lut [16].

The metabolites of iridoid are mainly phase 1 metabolites. The quasi-molecular ion peaks of *m/z* 449.1659 [M-H]$^-$ and *m/z* 405.1397 [M-H]$^-$ were observed in M3 and M5, respectively, which showed a mass increase of 16 Da compared with the corresponding ions of 8-O ASME and Log, and the same rules were found in the ion fragments. Therefore, it was concluded that they were the oxidation products of 8-O ASME and Log [17].

The quasi-molecular ion peak at *m/z* 402.1159 [M-H]$^-$ and the fragmentation ion at *m/z* 226.0839 [M-H-$C_6H_8O_6$]$^-$, corresponding to the aglycon of geniposide, were observed in M4. Subsequently, one molecule of H_2O was eliminated resulting in *m/z* 208.0733 [M-H-$C_6H_8O_6$-H_2O]$^-$ and one molecule of CH_3COOH was lost resulting in *m/z* 148.0519 [M-H-$C_6H_8O_6$-H_2O-CH_3COOH]$^-$. In agreement with the results of Han et al. it can be concluded that this metabolite is the glucuronidation product of geniposide [18].

3.3. Network pharmacological analysis of LH treatment for LF

The prototype and metabolic compounds in blood were selected for further analysis, and the relevant targets of compounds for the treatment of LF were predicted through the database. KEGG and GO enrichment analysis of the relevant targets was performed through the DAVID database.

We identified 124 common targets among 2132 LF-related targets and 303 chemical component-related targets (Fig. 6-A). Through network interaction analysis, it was implicated that Lut, geniposide, Log A, Log, 8-O ASME, SME and part of the metabolic components were the potential active ingredients in LH for the treatment of LF (Fig. 6-B). PI3K-Akt signaling pathway, FoxO signaling pathway, Ras signaling pathway are listed as signaling pathways containing more low-p-value genes, and these pathways contain most of the targets, including CA2, SRC, EGFR, IL-6, HMOX1, NQO-1, IL-18, MMPs and so on, which are highly associated with inflammation, oxidation and matrix formation (Fig. 6-C, D). These results suggest that Log A, Log, 8-O ASME and other compounds in LH may alleviate LF by alleviating inflammatory factors, reducing matrix formation, and antioxidative effects.

Table 1
Prototype compounds enter-into blood in LH.

No.	RT (min)	Molecular formula	MW	Adduct ion	Error (ppm)	Fragment ion	Identified compound	Type
1	3.024	$C_{17}H_{24}O_{11}$	449.1295	+HCOO	0.9	241.0737[M-H-$C_6H_{10}O_5$]$^-$	Phlorigidoside C	I
2	3.130	$C_{17}H_{24}O_{12}$	465.1244	+HCOO	3.9	257.0641[M-H-$C_6H_{10}O_5$]$^-$	Sesamoside	I
3	3.557	$C_{17}H_{26}O_{11}$	451.1452	+HCOO	-0.2	243.0882[M-H-$C_6H_{10}O_5$]$^-$ 225.0803[M-H-$C_6H_{10}O_5$-H_2O]$^-$	Shanzhiside Methylester	I
4	3.770	$C_{16}H_{24}O_{10}$	375.1291	-H	2.1	213.0780[M-H-$C_6H_{10}O_5$]$^-$	Loganic Acid	I
5	4.511	$C_{17}H_{24}O_{11}$	449.1295	+HCOO	2.7	241.0726[M-H-$C_6H_{10}O_5$]$^-$	7,8-Dehydropenstemoside	I
6	4.624	$C_{17}H_{24}O_{10}$	433.1346	+HCOO	3.0	225.0751[M-H-$C_6H_{10}O_5$]$^-$	Geniposide	I
7	4.838	$C_{17}H_{24}O_{10}$	433.1346	+HCOO	2.3	225.0775[M-H-$C_6H_{10}O_5$]$^-$	7-dehydroxy-2-zaluzioside	I
8	5.009	$C_{17}H_{26}O_{11}$	451.1452	+HCOO	-3.2	243.0896[M-H-$C_6H_{10}O_5$]$^-$	Penstemoside	I
9	5.493	$C_{17}H_{26}O_{10}$	435.1503	+HCOO	-1.6	227.0966[M-H-$C_6H_{10}O_5$]$^-$	Loganin	I
10	6.290	$C_{16}H_{24}O_9$	359.1342	-H	-0.2	359.1350[M-H]$^-$ 197.0810[M-H-$C_6H_{10}O_5$]$^-$	8-Epideoxyloganic Acid	I
11	6.410	$C_{19}H_{28}O_{12}$	493.1552	+HCOO	-0.8	868.3947[2 M-H]$^-$ 285.0974[M-H-$C_6H_{10}O_5$]$^-$	8-O-Acetyl shanzhiside methyl ester	I
12	10.844	$C_{15}H_{10}O_6$	285.0399	-H	1.0	285.0395[M-H]$^-$	Luteolin	F

Table 2
Metabolism compounds enter-into blood in LH.

No.	RT (min)	Molecular formula	MW	Adduct ion	Error (ppm)	Fragment ion	Prototype compound	Metabolic type
M1	3.315	$C_{18}H_{26}O_{12}$	433.1346	-H	4.6	271.0844[M-H-$C_6H_{11}O_5$]$^-$ 241.0698[M-H-$C_6H_{11}O_5$-OCH_2]$^-$	8-O-Acetyl shanzhiside methyl ester	Demethylation
M2	5.051	$C_{27}H_{26}O_{18}$	637.1041	-H	1.2	461.0720[M-H-$C_6H_8O_6$]$^-$ 285.0411[M-H-$C_6H_8O_6$-$C_6H_8O_6$]$^-$	Luteolin	Double glucuronidation
M3	5.286	$C_{19}H_{30}O_{12}$	449.1659	-H	1.6	287.1131[M-H-$C_6H_{11}O_5$]$^-$	8-O-Acetyl shanzhiside methyl ester	Oxidation
M4	5.351	$C_{17}H_{26}O_{11}$	402.1162	-H	1.2	226.0839[M-H-$C_6H_8O_6$]$^-$ 208.0733[M-H-$C_6H_8O_6$-H_2O]$^-$	Geniposide	Glucuronidation
M5	5.358	$C_{17}H_{26}O_{11}$	405.1397	-H	-2.7	242.0818[M-H-$C_6H_{11}O_5$]$^-$	Loganin	Oxidation
M6	6.752	$C_{21}H_{18}O_{15}S$	541.0288	-H	-1.8	364.9992[M-H-$C_6H_8O_6$]$^-$ 285.0393[M-H-SO_3-$C_6H_8O_6$]$^-$	Luteolin	Sulfation and glucuronidation
M7	7.933	$C_{21}H_{18}O_{12}$	461.0720	-H	-0.8	285.0410[M-H-$C_6H_8O_6$]$^-$	Luteolin	Glucuronidation
M8	9.613	$C_{22}H_{20}O_{12}$	475.0877	-H	0.4	299.0597[M-H-$C_6H_8O_6$]$^-$ 285.0410[M-H-$C_6H_8O_6$-CH_2]$^-$	Luteolin	Methylglucuronidation
M9	10.744	$C_{15}H_{10}O_9S$	364.9967	-H	-1.1	285.0389[M-H-SO_3]$^-$	Luteolin	Sulfation

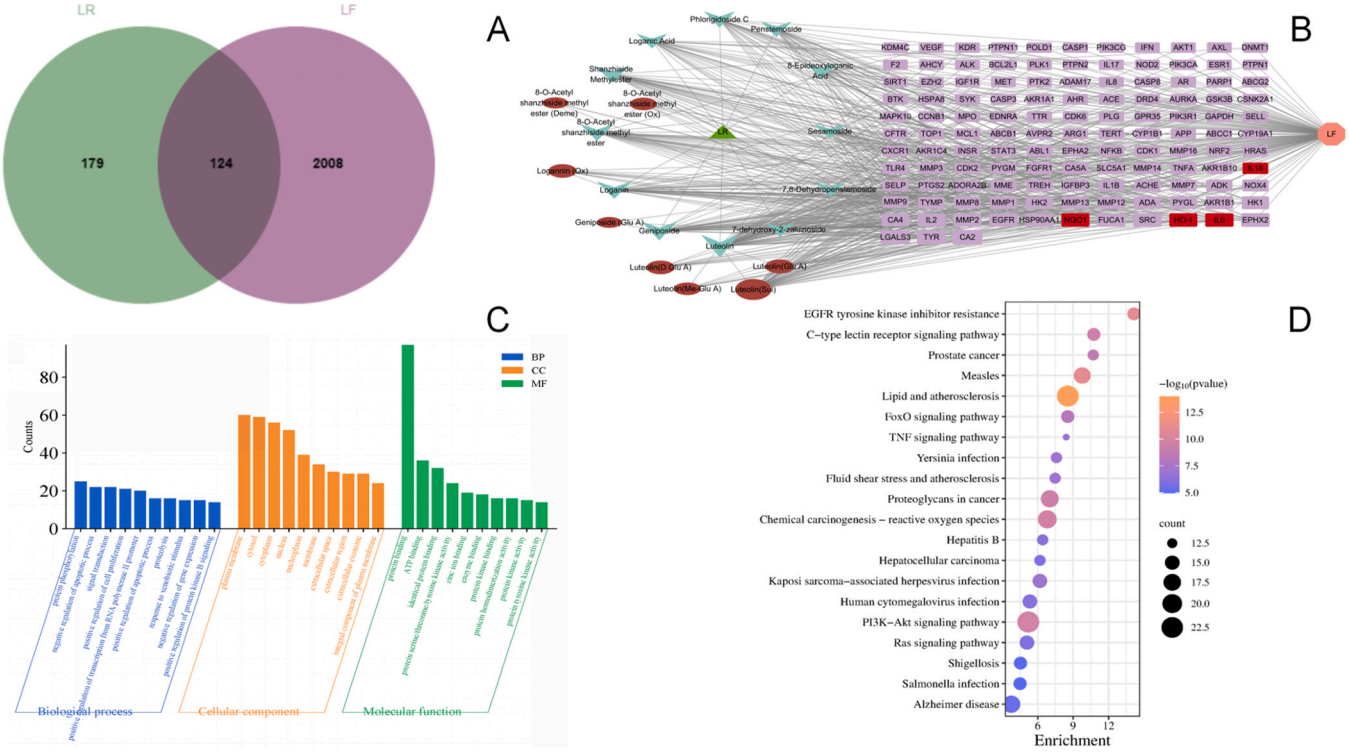

Fig. 6. Network pharmacological analysis based on prototype chemical components entering plasma. (A: Venn diagram illustrating the common targets of LF and LH; B: Network topology diagram depicting the active ingredient-target interactions; C: Bar chart presenting the results of GO enrichment analysis; D: Bubble diagram displaying the top 20 KEGG signaling pathways).

3.4. LH decreased LF related protein expression levels

According to the results of network pharmacology analysis, the author selected five compounds with a higher degree-value to examine their effects on LF. We stimulated HSC-T6 cells with TGF-β1 and interfered with five compounds and LH aqueous extracts of different concentrations. Compared with the control group, the protein expression of LN, Col-IV, PC-III and α-sma in the model group were significantly increased ($P < 0.01$). Compared with model group, 8-O ASME, Log A and Lut extremely significantly reduce the expression of Col-IV ($P < 0.01$). Log A, Log and Lut dramatically decrease the PC-III expression ($P < 0.05$). SME, Log, Log A and Lut sharply dwindle the LN expression ($P < 0.05$). SME, 8-O ASME, Log and Lut substantially lessen the expression of α-sma ($P < 0.05$). In addition, LH diminished the secretion of LN, Col-IV, PC-III and α-sma in a dose-dependent manner, and the high dose group (LH-H) showed eminently considerable differences (Fig. 7-A). Therefore, the high-dose group was selected for subsequent qRT-PCR experiments.

3.5. Mechanism of LH inhibiting HSC-T6 activation induced by TGF-β_1

To explore the mechanism of action of LH and its chemical constituents in alleviating LH, the gene expression levels of HO-1, NQO-1, IL-6, IL-18, COL3A1 and COL1A1 were detected by qRT-PCR in the same cell model.

The results demonstrated that, compared to the control group, the model group exhibited a marked down-regulation of gene expression for NQO-1 and HO-1 ($P < 0.01$). Among the five chemical components tested, both SME and Lut displayed a remarkable ability to enhance the gene expression of HO-1 ($P < 0.01$), while all five components were

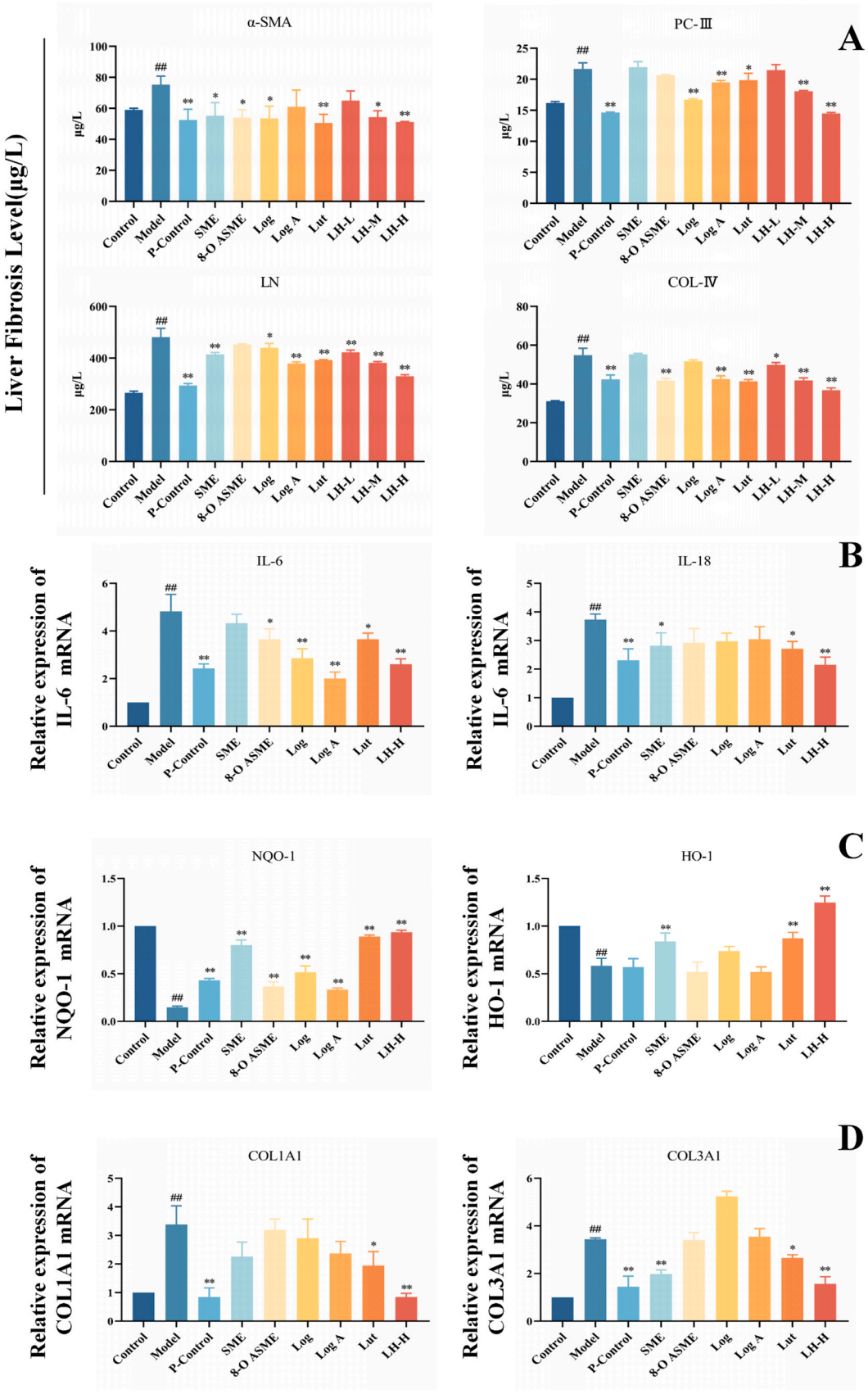

Fig. 7. Results of ELISA and qRT-PCR experiments. Data were presented as the mean ± SD (n = 3). $^{\#}P < 0.05$, $^{\#\#}P < 0.01$ vs. the Control group; $^{*}P < 0.05$, $^{**}P < 0.01$ vs. the Model group. (A: Expression levels of LN, Col-IV, PC-III and α-sma in different groups; B: Relative expression of NQO-1 and HO-1; C: Relative expression of IL-6 and IL-18; D: Relative expression of COL1A1 and COL3A1).

significantly up-regulated on HO-1 gene expression. Compared with the monomeric components, LH increased the gene expression of NQO-1 and HO-1 more significantly (Fig. 7-B).

In the gene expression assay of IL-18 and IL-6, the gene expression of model group was significantly higher than that of control group ($P < 0.01$). SME and Lut could substantially reduce the gene expression of IL-18 ($P < 0.05$), while 8-O ASME, Log, Log A and Lut could greatly decrease the gene expression of IL-6 ($P < 0.05$). The gene expression of IL-6 and IL-18 was enormously down-regulated by LH, exhibiting a superior effect compared to the monomer group ($P < 0.01$) (Fig. 7-C).

Compared to the control group, the model group exhibited a great upregulation in gene expressions of COL1A1 and COL3A1 ($P < 0.01$). Treatment with Lut resulted in a significant reduction in COL1A1 gene expression ($P < 0.05$), and SME and Lut significantly decreased gene expression of COL3A1 ($P < 0.05$). LH can markedly down-regulate the gene expression of COL1A1 and COL3A1, and the effect is better than that of monomer administration group ($P < 0.01$) (Fig. 7-D).

3.6. HE staining result

In the control group, hepatocytes were polygonal with round nuclei centrally located within the cells. Hepatic cords were arranged radially around the central vein, while maintaining a uniform hepatic sinusoidal space. No inflammatory cell infiltration or hepatocyte necrosis was found in the tissue, and the morphological structure of the tissue was normal. In the model group, a significant presence of venous congestion was observed in the liver tissue, along with pronounced connective tissue hyperplasia in the central vein and portal area, resulting in fibrous bridging, accompanied by a large number of lymphocyte infiltration. Hepatocytes showed punctate necrosis, karyopyknosis, microvacancy in the cytoplasm, and hepatocyte steatosis. Compared with the model group, the areas of hepatocyte and hepatic sinusoidal capsule hyperplasia, connective tissue hyperplasia and lymphocyte infiltration in the central vein and portal area, steatosis, and venous congestion area were reduced in each treatment group. LH reduced the LF area in a dose-dependent manner, and the effect of LH-H and SME was more significant, similar to that of the control group (Fig. 8).

4. Discussion

LF is a diffuse excessive deposition of extracellular matrix in the liver caused by viral infections, lipid accumulation, cholestasis and other exogenous factors. It represents a complex pathophysiological process underlying various liver diseases [3]. TCM shows promise for LF management due to its multi-component and multi-target treatment approach. However, since therapeutic effects can only be exerted by TCM components absorbed into the bloodstream, this study aims to elucidate the bioactive components of LH in LF treatment by analyzing its constituents and their absorption into the bloodstream.

The article identifies 50 compounds in the water extract of LH, including 19 phenylpropanoids, 20 iridoids, 9 flavonoids and 2 other compounds. Among these compounds, 11 iridoids and 1 flavonoid compound entered the blood as prototypes, which is related to the special structure of iridoid, rich hydroxyl group and special terpenoid structure to make it have higher bioavailability [19]. Following intestinal absorption, these compounds enter the hepatic portal vein through capillaries. However, phenylpropanes are not detected in blood samples due to their susceptibility to first-pass metabolism which limits their systemic circulation [20]. After entering the hepatic circulation via the hepatic portal vein, compounds will undergo one-phase metabolism under the action of enzyme metabolism, while compounds with poor water solubility require two-phase metabolism, combine with endogenous binders and then be excreted. This observation may explain why metabolites of iridoids primarily undergo one-phase metabolism while flavonoid metabolites predominantly involve two-phase metabolism such as glucuronidation [21,22].

The migrating components of the prototype and the metabolism in blood were selected as the research subjects for network pharmacology analysis. Experiment results demonstrated that the key active ingredients in LH include Lut, geniposide, Log A, Log, 8-O-ASME and SME. These ingredients primarily target inflammation, oxidative stress, and matrix metalloproteinases. Notably, certain metabolites were also associated with multiple targets, such as the sulfatation and glucuronidation products of Lut, and oxidation products of Log. SME alleviates depression by inhibiting LPS-induced upregulation of inflammatory factors in BV2 cells through regulation of the SOCS1/JAK2/STAT3 signaling pathway [23]. 8-O ASME can block the activation of microglia, relieve the phosphorylation of JNK, NFKB and TNF to inhibit anxiety, and regulate Nrf/HO-1 pathway by interfering with NLRP3-mediated inflammatory response, thus alleviating anxious insomnia caused by oxidative stress [24]. Log alleviated the progression of nonalcoholic steatohepatitis by blocking the formation of apoptosis-related proteins containing the caspase recruitment domain and disrupting the assembly of the NLRP3 inflammasome complex [25]. Log A attenuates the expansion of MnSOD, reduces the expression of ROS, inhibits the inactivation of MMP-9/2, and ultimately prevents epithelial mesenchymal transformation (A key pathway for myofibroblast production) [26]. Studies have shown that Lut can reduce ethanol-induced phosphorylation of SREBP protein and reduce AMP protein kinase, consequently improving lipid accumulation and overexpression of related genes in the liver, thus blocking the progression from alcoholic fatty liver to LF [27]. Studies have found that luteolin-7-O-glucuronide can be absorbed by the liver and reduce the expression of inflammatory factors in liver cells [28].

Based on the results of KEGG enrichment analysis, it was found that these compounds mainly regulate LF through PI3K-Akt signaling pathway, Ras signaling pathway and FoxO signaling pathway. PI3K-Akt signaling pathway can be activated by inflammatory factors,

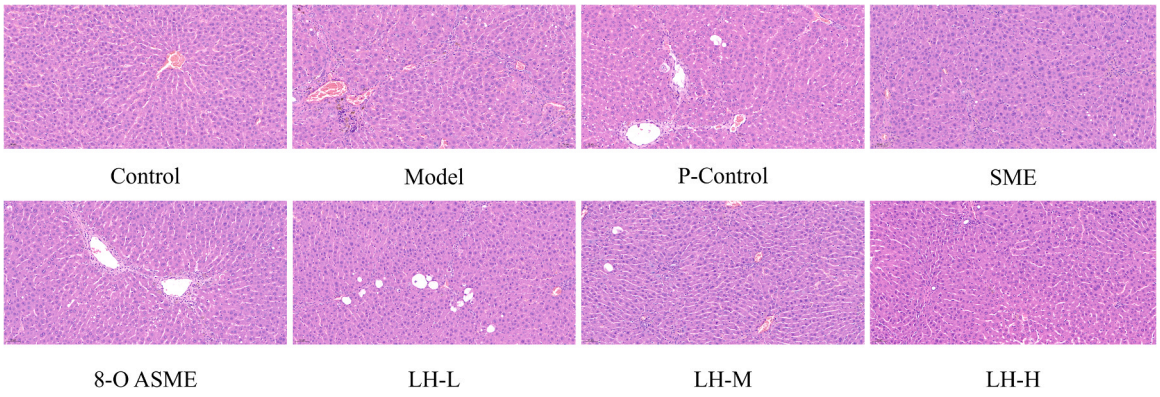

Fig. 8. HE staining results of rat liver tissue.

chemokines, growth factors and other signaling factors, participating in the response of cells to cell signals, promoting metabolism, proliferation, cell survival, growth and angiogenesis and other processes. Zhan et al. found that the total flavonoids in LH could reverse the changes of PI3K, p-Akt, p-Bad, Bcl-xL and Bcl-2 levels in ankle synovium of rats with rheumatoid arthritis. By inhibiting the level of IL-6 and IL-17 protein, the PI3K/Akt/Bad signaling pathway is inhibited to regulate apoptosis in the treatment of rheumatoid arthritis [5]. Although network pharmacological predictions indicate that most iridoid terpenes are key components regulating these signaling pathways, less research has been reported on their treatment of LF. Therefore, we analyzed their possibility to treat LF. Their effects, especially 8-O ASME and SME, on neurological disorders such as anxiety and depression have been confirmed [5]. The gut-liver-brain axis plays an irreplaceable role in the development of various diseases. Changes in glycolysis induced by depression also play a role in the phenotypic transformation of HSCs. In addition, the bacterial diversity and systemic inflammation caused by hepatic encephalopathy will promote LF progression [29].

Geniposide, as one of the active ingredients predicted by network pharmacology, was found to be able to act on multiple targets, but in another of our studies, geniposide failed to appear in every batch and origin [11]. Apart from this, although some metabolites can be associated with multiple targets, we cannot accurately determine the configuration of these isomers, and configuration and efficacy are closely related, so we did not select these compounds for subsequent experiments. Therefore, we chose Lut, Log A, Log, 8-O ASME and SME as research objects for subsequent experimental verification. IL-6, IL-18, HO-1 and NQO-1 have higher degree values and are involved in the regulation of multiple pathways.

Persistent oxidative stress, resulting from an imbalance between ROS production and antioxidant scavenging, is a critical mechanism in the progression of LF [30]. ROS can activate HSCs through histone modification, gene silencing and DNA methylation, leading to extracellular matrix (ECM) secretion, particularly type I collagen deposition, thereby exacerbating LF [31]. HO-1 and NQO1, key enzymes involved in ROS detoxification, are upregulated when Nrf2 activation is uncoupled from Keap1 [32]. In our study, we observed that LH and its monomeric components upregulate the expression of HO-1 and NQO-1, which may be related to the activation of Nrf2. Previous experiments have also demonstrated the ability of LH components to activate Nrf2, thereby reducing oxidative stress-induced injury by attenuating neuronal apoptosis and ameliorating cognitive impairment [24,33].

In addition, the lack of Nrf2 results in increased IKKβ activity, which promotes the phosphorylation and degradation of IκBα, subsequently activating NF-κBp50 to enter the nucleus [34]. Activation of NF-κB can enhance the transcription of IL-18 precursor and secretion of IL-6, thereby exacerbating inflammation [35]. These pro-inflammatory factors stimulate surrounding HSCs to activate and induce excessive ECM deposition [2]. Our study confirmed that LH and its monomer reduced IL-18 and IL-6 secretion through potential mediation of the Nrf2/NF-κB cascade. This led to a significant reduction in collagen secretion and other ECM-related proteins due to improved oxidative stress and inflammation levels.

Although the inhibitory effect of LH and its monomer on HSC activation has been demonstrated in vitro, it is essential for the drug to reach a certain threshold of absorption in order to exert its pharmacological efficacy. We confirmed that LH and its monomer components SME and 8-O ASME could significantly reduce collagen area and fibrous bridging in liver tissue by gavage administration of human equivalent dose of LH to rats.

The results presented here provide evidence for the chemical components associated with the pharmacological properties of LH in the treatment of LF and offer preliminary insights into its mechanism of action. Subsequently, we will verify these active ingredients in vivo and investigate whether the index components 8-O ASME and SME in LH can produce the same mechanism of action as predicted in complex organisms. These research results will serve as fundamental data for establishing and improving the quality standard of LH, while also providing a theoretical basis for further exploration of its active ingredients and clinical effects.

5. Conclusion

Lut, SME, Log A, Log and 8-O ASME are the effective active ingredients of LH in the treatment of LF, and they may improve LF by mediating Nrf2/NF-κB pathway to exert antioxidant and anti-inflammatory effects and inhibit ECM production.

Funding

This study was funded by Tianjin Science and Technology Plan Project (21ZYCGSN00660).

CRediT authorship contribution statement

Jiaming Ge: Writing – review & editing, Writing – original draft, Formal analysis, Conceptualization. **Weisan Chen:** Writing – review & editing, Writing – original draft. **Jinlong Yang:** Writing – review & editing, Methodology. **Mengyuan Li:** Writing – review & editing, Resources. **Jing Zhao:** Writing – original draft, Investigation. **Ying Zhao:** Writing – review & editing, Investigation. **Tianbao Song:** Supervision, Investigation. **Xiankuan Li:** Writing – original draft, Resources, Methodology, Funding acquisition. **Jiali Ren:** Software. **Xinchen Gao:** Methodology.

Declaration of Competing Interest

The authors declare that they have no known competing financial interests or personal relationships that could have appeared to influence the work reported in this paper.

Appendix A. Supporting information

Supplementary data associated with this article can be found in the online version at doi:10.1016/j.jpba.2024.116204.

References

[1] T. Kisseleva, D. Brenner, Molecular and cellular mechanisms of liver fibrosis and its regression, Nat. Rev. Gastroenterol. Hepatol. 18 (2021) 151–166.
[2] N. Roehlen, E. Crouchet, T.F. Baumert, Liver fibrosis: mechanistic concepts and therapeutic perspectives, Cells 9 (2020) 875.
[3] V. Hernandez-Gea, S.L. Friedman, Pathogenesis of liver fibrosis, Annu. Rev. Phytopathol. 6 (2011) 425–456.
[4] H. Li, Advances in anti hepatic fibrotic therapy with traditional Chinese medicine herbal formula, J. Ethnopharmacol. 251 (2020) 112442.
[5] Y. Li, F. Li, T.T. Zheng, L. Shi, Z.G. Zhang, T.M. Niu, Q.Y. Wang, D.S. Zhao, W. Li, P. Zhao, Lamiophlomis herba: A comprehensive overview of its chemical constituents, pharmacology, clinical applications, and quality control, Biomed. Pharmacother. 144 (2021) 112299.
[6] G. Wan, Z. Chen, L. Lei, X. Geng, Y. Zhang, C. Yang, W. Cao, Z. Pan, The total polyphenolic glycoside extract of Lamiophlomis rotata ameliorates hepatic fibrosis through apoptosis by TGF-β/Smad signaling pathway, Chin. Med. 18 (2023) 20.
[7] C. Yang, X. Geng, G. Wan, L. Song, Y. Wang, G. Zhou, J. Wang, Z. Pan, Transcriptomic and proteomic investigation of the ameliorative effect of total polyphenolic glycoside extract on hepatic fibrosis in Lamiophlomis rotata Kudo via the AGE/RAGE pathway, J. Ethnopharmacol. 324 (2024) 117720.
[8] D.M. Xiang, W. Sun, B.F. Ning, T.F. Zhou, X.F. Li, W. Zhong, Z. Cheng, M.Y. Xia, X. Wang, X. Deng, W. Wang, H.Y. Li, X.L. Cui, S.C. Li, B. Wu, W.F. Xie, H.Y. Wang, J. Ding, The HLF/IL-6/STAT3 feedforward circuit drives hepatic stellate cell activation to promote liver fibrosis, Gut 67 (2018) 1704–1715.
[9] J. Knorr, B. Kaufmann, M.E. Inzaugarat, T.M. Holtmann, L. Geisler, J. Hundertmark, M.S. Kohlhepp, L.M. Boosheri, D.R. Chilin-Fuentes, A. Birmingham, K.M. Fisch, J.D. Schilling, S.H. Loosen, C. Trautwein, C. Roderburg, M. Demir, F. Tacke, H.M. Hoffman, A.E. Feldstein, A. Wree, Interleukin-18 signaling promotes activation of hepatic stellate cells in mouse liver fibrosis, Hepatology 77 (2023) 1968–1982.

[10] J. Lee, J.W. Lim, H. Kim, Lycopene inhibits IL-6 expression by upregulating NQO1 and HO-1 via activation of Nrf2 in Ethanol/lipopolysaccharide-stimulated pancreatic acinar cells, Antioxid. 11 (2022) 519.
[11] J. Chen, J. Ge, W. Chen, Y. Zhao, T. Song, K. Fu, X. Li, Y. Zheng, UPLC-Q-TOF-MS based investigation into the bioactive compounds and molecular mechanisms of Lamiophlomis herba against hepatic fibrosis, Phytomedicine 121 (2023) 155085.
[12] L.J. Wang, Z.S. Zhao, Q.Y. Wang, Experimental study on toxicity of Lamiophlomis rotata, Lishizhen Med. Mater. Med. Res. 22 (2011) 256–257.
[13] M. La, F. Zhang, S. Gao, X. Liu, Z. Wu, L. Sun, X. Tao, W. Chen, Constituent analysis and quality control of Lamiophlomis rotata by LC-TOF/MS and HPLC-UV, J. Pharm. Biomed. Anal. 102 (2015) 366–376.
[14] L. Wu, L. Li, M. Wang, C. Shan, X. Cui, J. Wang, N. Ding, D. Yu, Y. Tang, Target and non-target identification of chemical components in Lamiophlomis rotata by liquid chromatography/quadrupole time-of-flight mass spectrometry using a three-step protocol, Rapid Commun. Mass Spectrom. 30 (2016) 2145–2154.
[15] L. Zhang, C.X. Wang, J. Wu, T.Y. Wang, Q.Q. Zhong, Y. Du, S. Ji, L. Wang, M. Z. Guo, S.Q. Xu, D.Q. Tang, Metabolic profiling of mice plasma, bile, urine and feces after oral administration of two licorice flavonones, J. Ethnopharmacol. 257 (2020) 112892.
[16] N. Hayasaka, N. Shimizu, T. Komoda, S. Mohri, T. Tsushida, T. Eitsuka, T. Miyazawa, K. Nakagawa, Absorption and metabolism of luteolin in rats and humans in relation to in vitro anti-inflammatory effects, J. Agric. Food Chem. 66 (2018) 11320–11329.
[17] Y. Wang, S. Chen, J. Mo, X. Chen, Y. Yang, K. Zhang, Z. Chen, C.X. Zhang, Investigate the metabolic profile and potential active compounds of Fructus Corni in the treatment of heart failure by applying ultra-performance liquid chromatography with quadrupole time-of-flight mass spectrometry and network pharmacology, J. Sep. Sci. 45 (2022) 4348–4363.
[18] H. Han, L. Yang, Y. Xu, Y. Ding, S.W. Bligh, T. Zhang, Z. Wang, Identification of metabolites of geniposide in rat urine using ultra-performance liquid chromatography combined with electrospray ionization quadrupole time-of-flight tandem mass spectrometry, Rapid Commun. Mass Spectrom. 25 (2011) 3339–3350.
[19] Y. Kou, Z. Li, T. Yang, X. Shen, X. Wang, H. Li, K. Zhou, L. Li, Z. Xia, X. Zheng, Y. Zhao, Therapeutic potential of plant iridoids in depression: a review, Pharm. Biol. 60 (2022) 2167–2181.
[20] F.J. Olivas-Aguirre, S. Mendoza, E. Alvarez-Parrilla, G.A. Gonzalez-Aguilar, M. A. Villegas-Ochoa, J.T.Y. Quintero-Vargas, A. Wall-Medrano, First-pass metabolism of polyphenols from selected berries: a high-throughput bioanalytical approach, Antioxid. 9 (2020) 311.
[21] A. Gradolatto, M.C. Canivenc-Lavier, J.P. Basly, M.H. Siess, C. Teyssier, Metabolism of apigenin by rat liver phase I and phase ii enzymes and by isolated perfused rat liver, Drug Metab. Dispos. 32 (2004) 58–65.
[22] Z. Xiang, S. Wang, H. Li, P. Dong, F. Dong, Z. Li, L. Dai, J. Zhang, Detection and identification of catalpol metabolites in the rat plasma, urine and faeces using ultra-high performance liquid chromatography-Q exactive hybrid quadrupole-orbitrap high-resolution accurate mass spectrometry, Curr. Drug Metab. 22 (2021) 173–184.
[23] Z. Sun, H. Zhan, C. Wang, P. Guo, Shanzhiside methylester protects against depression by inhibiting inflammation via the miRNA-155-5p/SOCS1 axis, Psychopharmacol. 239 (2022) 2201–2213.
[24] Y.J. Li, X.L. He, J.Y. Zhang, X.J. Liu, J.L. Liang, Q. Zhou, G.H. Zhou, 8-O-acetyl shanzhiside methylester protects against sleep deprivation-induced cognitive deficits and anxiety-like behaviors by regulating NLRP3 and Nrf2 pathways in mice, Metab. Brain Dis. 38 (2023) 641–655.
[25] Y.C. Cheng, L.W. Chu, J.Y. Chen, S.L. Hsieh, Y.C. Chang, Z.K. Dai, B.N. Wu, Loganin attenuates high glucose-induced schwann cells pyroptosis by inhibiting ROS generation and NLRP3 inflammasome activation, Cells 9 (2020) 1948.
[26] N.Y. Kim, I.J. Ha, J.Y. Um, A.P. Kumar, G. Sethi, K.S. Ahn, Loganic acid regulates the transition between epithelial and mesenchymal-like phenotypes by alleviating MnSOD expression in hepatocellular carcinoma cells, Life Sci. 317 (2023) 121458.
[27] G. Liu, Y. Zhang, C. Liu, D.Q. Xu, R. Zhang, Y. Cheng, Y. Pan, C. Huang, Y. Chen, Luteolin alleviates alcoholic liver disease induced by chronic and binge ethanol feeding in mice, J. Nutr. 144 (2014) 1009–1015.
[28] A. Kure, K. Nakagawa, M. Kondo, S. Kato, F. Kimura, A. Watanabe, N. Shoji, S. Hatanaka, T. Tsushida, T. Miyazawa, Metabolic fate of luteolin in rats: its relationship to anti-inflammatory effect, J. Agric. Food Chem. 64 (2016) 4246–4254.
[29] V.T. Kronsten, D.L. Shawcross, Hepatic encephalopathy and depression in chronic liver disease: is the common link systemic inflammation? Anal. Biochem. 636 (2022) 114437.
[30] Y. Gong, Y. Yang, Activation of Nrf2/AREs-mediated antioxidant signalling, and suppression of profibrotic TGF-β1/Smad3 pathway: a promising therapeutic strategy for hepatic fibrosis - a review, Life Sci. 256 (2020) 117909.
[31] S. Li, M. Hong, H. Tan, N. Wang, Y. Feng, Insights into the role and interdependence of oxidative stress and inflammation in liver diseases, Oxid. Med. Cell. Longev. 2016 (2016) 4234061.
[32] E. Catanzaro, C. Calcabrini, E. Turrini, P. Sestili, C. Fimognari, Nrf2: a potential therapeutic target for naturally occurring anticancer drugs? Expert Opin. Ther. Targets 21 (2017) 781–793.
[33] M. Xia, Y. Zhang, H. Wu, Q. Zhang, Q. Liu, G. Li, T. Zhao, X. Liu, S. Zheng, Z. Qian, H. Li, Forsythoside B attenuates neuro-inflammation and neuronal apoptosis by inhibition of NF-κB and p38-MAPK signaling pathways through activating Nrf2 post spinal cord injury, Int. Immunopharmacol. 111 (2022) 109120.
[34] J.D. Wardyn, A.H. Ponsford, C.M. Sanderson, Dissecting molecular cross-talk between Nrf2 and NF-κB response pathways, Biochem. Soc. Trans. 43 (2015) 621–626.
[35] G. Kaplanski, Interleukin-18: biological properties and role in disease pathogenesis, Immunol. Rev. 281 (2018) 138–153.